Appl. Phys. B 62, 421–426 (1996)

Applied Physics B Lasers and Optics

Origin and manifestation of the anharmonic potential felt by an ion-cloud in an actual Paul trap

X. Luo, X. Zhu, K. Gao, J. Li, M. Yan, L. Shi, J. Xu

Laboratory of Magnetic Resonance and Atomic and Molecular Physics, Wuhan Institute of Physics, The Chinese Academy of Sciences, Wuhan, 430071, People's Republic of China
(Fax: + 86-27/788-5291)

Received: 6 May 1994/Accepted: 5 July 1995

Abstract. The anharmonic potential felt by a single-species ions confined in a rf quadrupole trap which results from a non-ideal trap configuration and the charge distribution of the ion cloud is studied. The rf resonance-absorption spectra are explained by a Duffing oscillator and a representation of the line-shape parameter η is derived. For $\eta > 0.77$, the electric signals will exhibit hysteresis. The relation with the anharmonic potential is discussed.

PACS: 29.25; 32.80.Pj; 35.80

The ion trap has been a fundamental experimental tool for precision measurements of the mass energy levels and motional frequencies of charged particles and for quantum physics studies during past decades [1, 2]. For most precision measurements, it is desirable that the charged particles move harmonically under the action of a pure quadrupole potential in the trap in order to obtain a narrow, unshifted and distortion-free (usually Lorentzian) line shape of signals [3]. An ideal quadrupole trap with three flawless and infinitely extended hyperboloid electrodes supplied with a dc voltage certainly meets this requirement. However, for the actual trap electrodes with inevitable truncation, holes and defects of mechanical fabrication and assembling, a small amount of higher-order potentials is necessarily superposed on the dominant quadrupole one. Elaborate adjustment of the voltages on the compensation electrodes [3] and the control of particle movement quite nearly around the trap center can eliminate most of the higher-order potential effects. For conventional traps without compensation, the existence of a tiny higher-order potential will generally result in anharmonicity of the ion motion, and thus line shift, broadening and distortion (e.g., hysteresis) of signals. Higher-order potentials will surely exist in cylindrical [4, 5], linear [6–8] and ring traps [9, 10], which were successfully applied for various studies, but they are not our concern in this paper.

For a single electron trapped in the Penning trap, the hysteresis of the anharmonic axial resonance due to the practical electrode imperfection and its elimination were studied [3], the hysteresis caused by the nonlinear relativistic cyclotron motion was also observed and explained [11, 12] and the anharmonicity induced by the presence of two different species of ions in a Paul trap had been demonstrated by Kajita et al. [13]. Recently, we reported on a preliminary observation of the hysteresis of the axial resonance of a single-species ion cloud confined in an actual Paul trap and gave a qualitative explanation by introducing a nonlinear coefficient phenomenologically [6]. To our knowledge, no quantitative analysis of the anharmonic potential for the ion cloud moving in the Paul trap has been given yet because of the difficulties in treating the time-dependent potential and the ion–ion interaction. The effects of other ions in the cloud, the so-called space charge, on an ion stored in both Penning and Paul traps were extensively investigated by various approaches [15–19], but the main concern of the previous studies was focused on modifications of ion frequencies, such as cyclotron and magnetron frequencies in the Penning trap [15] and secular axial and radial frequencies in the Paul trap [18, 19]. It is anticipated that the potential produced by the space charge with a complicated distribution, even its average, cannot be inclusively described by a pure quadrupole term, and that it should contribute somewhat to the anharmonicity. In this paper, we present a unified treatment of an anharmonic force which is felt by the ion cloud in a non-ideal Paul trap and originates from the imperfect electrode configuration and ion-charge distribution, and show the relationship between the experimental signals with hysteresis and the physical parameters of interest.

1 Extended pseudopotential model with an imperfect trap configuration

Ion confinement in a Paul trap is accomplished by a voltage $V = V_{dc} + V_{ac}\cos\Omega t$ applied to the electrodes. For an ideal trap configuration, this voltage will produce

a time-dependent quadrupole potential in the chamber [20]

$$\Phi(r,z;t) = -\frac{m\Omega^2}{16q}(a_z - 2q_z\cos\Omega t)(r^2 - 2z^2), \tag{1}$$

where m denotes the ion's mass, q the ion's charge, $a_z = -8qV_{dc}/mr_0^2\Omega^2$, $q_z = 4qV_{ac}/mr_0^2\Omega^2$ with r_0 being the radius of the trap's ring electrode, $z_0 = r_0/\sqrt{2}$, the half distance of the trap's end caps; V_{dc} and V_{ac}, the applied dc and ac voltages, respectively, $\Omega/2\pi$ is the trap's driving frequency, $r = \sqrt{x^2+y^2}$ and z are the radial and axial coordinates of the trap, respectively. The corresponding equation of motion for a single trapped ion is the Mathieu equation with well-known solutions [21].

In the limit of $|a_z| \ll |q_z| \ll 1$, Dehmelt described the motion of a single ion in the Paul trap with a pseudopotential model [22]. In this case, the axial displacement $z(t)$ of the motion is decomposed as:

$$z(t) = \bar{z}(t) + \xi(t) = \bar{z}(t) + \xi_0(\bar{z})\cos\Omega t, \tag{2}$$

where the displacement, $\bar{z}(t)$, of the axial macromotion or secular motion is governed by a time-averaged effective potential, namely, pseudopotential, and the superposed axial micromotion $\xi(t)$ is mainly the oscillation at the trap's driving frequency. From (1), the expression of the pseudopotential in the z-direction can be derived as

$$\Phi_{po}(\bar{z}) = \frac{1}{2q} m\omega_{iz}^2\bar{z}^2,$$

$$\text{with } \omega_{iz}^2 = \frac{1}{4}\Omega^2\beta_z^2 = \frac{1}{4}\Omega^2\left(a_z + \frac{q_z^2}{2}\right).$$

For an actual quadrupole trap with truncation, holes and other imperfections, we follow the approach given by Brown and Gabrielse [3] and assume a small octupole potential:

$$\Delta\Phi = \frac{V_{dc} + V_{ac}\cos\Omega t}{2}\frac{C_4}{z_0^4}\left(z^4 - 3z^2r^2 + \frac{3r^4}{8}\right) \tag{3}$$

as the leading anharmonic correction, where C_4 is the expanding coefficient in Lagendre polynomials, which indicates the scale of this octupole potential. The magnitude and sign of C_4 depend on the actual configuration of the trap and its absolute value is typically between 10^{-1} and 10^{-2} for the trap without compensation [3].

Following Dehmelt's approach, the extended pseudopotential created by time-dependent quadrupole and octupole potentials $\Phi(r,z;t) + \Delta\Phi$ is easily derived. Firstly, the dc voltage is supposed to be equal to zero and the coupling between the z and r directions is neglected [3]; then the force acting on an ion in the z-direction is

$$F_z(t) = \frac{qV_{ac}}{z_0^2} z(t)\left(1 - \frac{2C_4z^2(t)}{z_0^2}\right)\cos\Omega t \tag{4}$$

which produces a macromotion by an equivalent alternating electric field $E_0[z(t)]\cos\Omega t = -F_z(t)/q$ superposed by a micromotion with amplitude $\xi_0(\bar{z}) = qE_0(\bar{z})/m\Omega^2$. Expanding this inhomogeneous electric field at $\bar{z}$ to read

$$E_0[z(t)] = E_0(\bar{z}) + \left.\frac{\partial E_0}{\partial z}\right|_{z=\bar{z}}\xi + \frac{1}{2}\left.\frac{\partial^2 E_0}{\partial z^2}\right|_{z=\bar{z}}$$
$$\xi^2 + \frac{1}{6}\left.\frac{\partial^3 E_0}{\partial z^3}\right|_{z=\bar{z}}\xi^3 + \cdots\cdots,$$

we get an approximate expression for the average force experienced by an ion in a micromotion cycle

$$\langle F_z(t)\rangle_\Omega \approx -\frac{1}{8}m\Omega^2q_z^2\bar{z}\left[1 - \left(8 + \frac{3}{8}q_z^2\right)C_4\left(\frac{\bar{z}}{z_0}\right)^2\right].$$

Secondly, if the dc voltage is not equal to zero, it only contributes to the secular motion as it is time-independent. The total force controlling the macromotion in the axial direction is then deduced to be

$$F(\bar{z}) = -m\omega_{iz}^2\left[1 + \frac{8}{3}\lambda_{iz}\left(\frac{\bar{z}}{z_0}\right)^2\right]\bar{z}, \tag{5}$$

and the corresponding pseudopotential in the z-direction can be integrated as

$$\Phi_p(\bar{z}) = \frac{1}{2q}m\omega_{iz}^2\bar{z}^2\left[1 + \frac{4}{3}\lambda_{iz}^2\left(\frac{\bar{z}}{z_0}\right)^2\right] \tag{6}$$

with

$$\lambda_{iz} = -\frac{3}{4}C_4f_z(a_z,q_z) = -\frac{3}{4}C_4\frac{a_z + 2q_z^2 + 3q_z^4/32}{a_z + q_z^2/2}. \tag{7}$$

The expression for the pseudopotential in the r-direction can be obtained in a similar way.

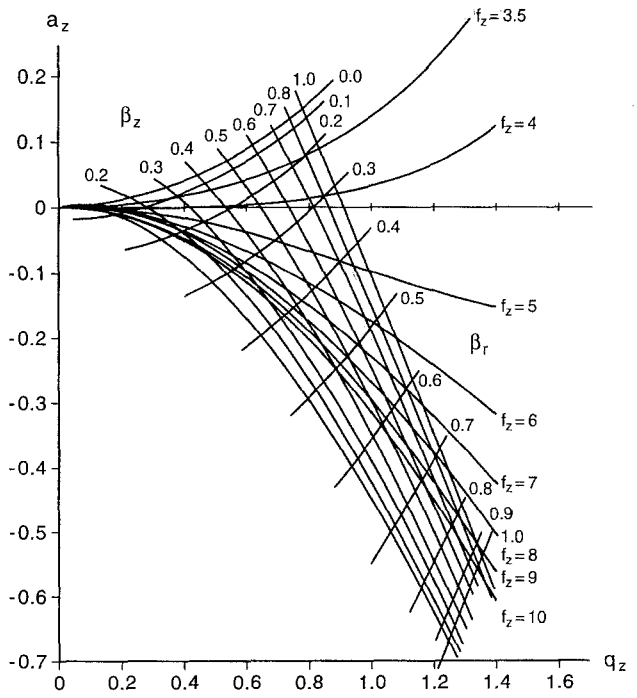

Fig. 1. The relationship between the anharmonic coefficient originating from imperfect trap configuration and operation parameters

It is obvious that this extended pseudopotential has not merely been a simple harmonic potential as there is a fourth-order term of $\bar{z}$ arisen. Because the pseudopotential describes the time-averaged effects of the confining voltage over a micromotion cycle, not only the harmonic but also the anharmonic term of this pseudopotential is related to the operating parameters a_z and q_z. From (7) we see that the introduced anharmonic coefficient λ_{iz} is directly proportional to octupole structural coefficient C_4 and varies with different operation parameters. When $V_{ac} = 0$, λ_{iz} is identical with that for a Penning trap [3], For an ideal trap configuration, C_4 is equal to zero and the anharmonic term of the pseudopotential vanishes; so, the secular motion of the trapped ion is dominated only by a harmonic potential. But the motion of an ion in a trap with imperfect configuration will exhibit the nonlinear characteristics which are scaled by λ_{iz}. In Fig. 1, a series of curves of iso-f_z is plotted, from which it can be seen that f_z is always positive in the first stability region and increases as q_z increases along a certain iso-β_z line. It is worth noting that the iso-f_z lines are valid only in the region of $|a_z| \ll |q_z| \ll 1$, although they are plotted in the whole stability chart.

2 Nonlinearity resulting from ion charge distribution

Ion clouds in Paul traps enjoy continuing interest because of its high signal-to-noise ratio due to the large ion number obtainable. However, this advantage is achieved at the cost of unavoidable asymmetric effects dominantly caused by the space-charge potential of the trapped ions. A self-consistent calculation of the distribution and energy of an ion cloud was given by Meis et al. [19]. They started with a spherical pseudopotential by means of restricting $a_z = -q^2/4$ and consequently $\omega_{iz} = \omega_{ir} = \omega_i = \Omega q_z/4$.

Supposing the ion cloud is in thermal equilibrium through a heating bath and then, with a Gaussian-like spherical distribution as

$$n(R) = n(0)\exp(-R^2/R_c^2), \tag{8}$$

where $n(0) = \pi^{2/3}N/R_c^3$ is the central density of the ion cloud, $R = \sqrt{r^2 + z^2}$ is the distance from the centre of the trap and R_c is the characteristic radius of the cloud scaling its dimension. Meis et al. solved Poisson's equation for the space-charge potential without angular dependence and obtained [19]

$$\Phi_{sc}(R) = \frac{qN}{4\pi\varepsilon_0 R}\,\mathrm{erf}(R/R_c).$$

Then, the total effective potential is

$$\Phi_t(R) = \frac{1}{2q}m\omega_i^2 R^2 + \frac{qN}{4\pi\varepsilon_0 R}\,\mathrm{erf}(R/R_c), \tag{9}$$

where the error function $\mathrm{erf}(x) = \frac{2}{\sqrt{\pi}}\int_0^x e^{-x^2}dx$.

In their opinion, the observed secular frequency was the mean value of the local frequency $\omega_m(R)$ averaged over the distribution (8) to read

$$\langle\omega_m(R)\rangle = \{\omega_i^2 - [q^2 n(0)|\mu|/m\varepsilon_0]\}^{1/2}$$

with $\mu = -0.23$. The effects of this charge distribution were all converted into the shift in the second-order term of the effective potential or the secular frequency.

In this paper, we concentrate on the motion of an ion cloud confined in the Paul trap detected by rf resonance absorption with an applied weak detection voltage $V_d\cos\omega t$ in the axial direction. As every ion in the cloud has about the same phase near resonance, the ion cloud maintains its distribution in motion. Hence, the motion of the ion cloud is similar to the motion of a single giant particle along the axis. The forces acting on the ion cloud mainly originate from the confining field and the Coulomb interaction between the ions. The effect of the confining field is approximately described by the pseudopotential, while the space-charge potential is determined by the ion distribution. Assuming that the centre of mass of the ion cloud is at z_c, corresponding to a distribution $n(\mathbf{R}, z_c) = n(0)\exp\{-[x^2 + y^2 - (z - z_c)^2]/R_c^2\}$, then the total energy of the cloud is

$$U(z_c) = \int q\Phi_t(R)n(\mathbf{R}, z_c)d^3\mathbf{R}. \tag{10}$$

Because the detection field is weak, the movement of the ion cloud along the z-axis is so small that $|z_c| \ll R_c$ is satisfied in most cases. By writing the error function $\mathrm{erf}(R/R_c)$ in powers of R/R_c and performing somewhat lengthy calculations, one obtains

$$\begin{aligned}
U(z_c) = C + \frac{1}{2}Nm\omega_i^2 z_c^2 + \frac{n(0)Nq^2}{2\pi^{3/2}\varepsilon_0} z_c^2 \Bigg\{ & \sum_{n=1}^{\infty} (-1)^n [(n-1)!(2n+1)R_c^{2n+1}]^{-1} \\
& \times \int R^{2(n-1)}\exp(-R/R_c^2)d^3R + \sum_{n=2}^{\infty}(-1)^n 2[(n-1)!(2n+1)R_c^{2n+1}]^{-1}\int z^2 R^{2(n-2)}\exp(-R^2/R_c^2)d^3\mathbf{R}\Bigg\} \\
+ \frac{n(0)Nq^2}{2\pi^{3/2}\varepsilon_0} z_c^4 \Bigg\{ & \sum_{n=2}^{\infty}(-1)^n [2(n-2)!(2n+1)R_c^{2n+1}]^{-1}\int R^{2(n-2)}\exp(-R^2/R_c^2)d^3R \\
& + \sum_{n=3}^{\infty}(-1)^n 2[(n-3)!(2n+1)R_c^{2n+1}]^{-1}\int z^2 R^{2(n-3)}\exp(-R^2/R_c^2)d^3R \\
& + \sum_{n=4}^{\infty}(-1)^n \frac{2}{3}[(n-4)!(2n+1)R_c^{2n+1}]^{-1}\int z^4 R^{2(n-4)}\exp(-R^2/R_c^2)d^3R\Bigg\} + \cdots,
\end{aligned}$$

where C is a constant not involving z_c and all terms of odd powers of z_c vanish because of symmetry. Calculating

these integrals and ignoring divergent infinite series[1], we obtain

$$U(z_c) \approx C' + \frac{1}{2} Nm\omega_i^2 z_c^2 - \frac{1}{2} Nm \frac{n(0)q^2}{m\varepsilon_0} |\mu| z_c^2 + \frac{1}{2} Nm \frac{n(0)q^2}{m\varepsilon_0 R_c^2} |\nu| z_c^4 + \cdots , \tag{11}$$

with

$$\mu' = \sum_{n=1}^{\infty} (-1)^n \frac{1}{(n-1)!(2n+1)} \times \frac{(2n-1)!!}{2^{n-1}} = -0.174,$$

$$\nu = \sum_{n=2}^{\infty} (-1)^n \frac{1}{(n-2)!(2n+1)} \times \frac{(2n-3)!!}{2^{n-1}} = -0.046.$$

The averaging force acting on each ion of this giant particle is

$$F(z_c) = -\frac{1}{N} \frac{\partial U(z_c)}{\partial z_c} = -m\omega_c^2 \left[1 + \frac{8}{3} \lambda_c \left(\frac{z_c}{R_c}\right)^2\right] z_c, \tag{12}$$

with

$$\omega_c^2 = \omega_i^2 - \frac{q^2 n(0)|\mu'|}{m\varepsilon_0} \tag{13}$$

and

$$\lambda_c = \frac{3n(0)q^2|\nu|}{4m\varepsilon_0\omega_c^2} (> 0). \tag{14}$$

It can be seen that the presence of the space charge not only shifts the central frequency ω_c of the ion cloud from the secular frequency ω_i calculated from the trap potential but also yields an anharmonic term scaling with λ_c. For the operating points with a given ω_i, the less the ion mass m and/or the higher the ion number N, which is proportional to $n(0)$ for a fixed R_c, the larger the frequency shift and λ_c. The values of ω_c and λ_c can be obtained from the operating parameters and $n(0)$ with the method given by Meis et al. [19].

In practice, the higher-order effects to the motion of the ion cloud in a Paul trap are caused by the non-ideal trap configuration and charge distribution together, which, in first-order approximation, are the superposition of these two effects. When the pseudopotential is isotropic, the anharmonic coefficient introduced by the imperfect trap configuration will become

$$\lambda_{iz} = -\frac{3}{4} C_4 f_z(a_z, q_z) \approx -\frac{21}{4} C_4 .$$

[1] They are negligible physically because the displacement of the ion cloud is small or $|z_c| \ll R_c$; mathematically z_c is but a virtual displacement and we take the limit $z_c \to 0$ to advance

Taking this into account, from a similar treatment we get the total central frequency and the total anharmonic coefficient as

$$\omega_{ct}^2 \approx \omega_i^2 \left(1 - 21C_4 \frac{R_c^2}{z_0^2} - \frac{q^2 n(0)|\mu|}{m\varepsilon_0\omega_i^2}\right) \tag{15}$$

and

$$\lambda_{ct} \approx \frac{3n(0)q^2|\nu|}{4m\varepsilon_0\omega_c^2} - \frac{21}{4} C_4 \frac{\omega_i^2 R_c^2}{\omega_c^2 z_0^2}, \tag{16}$$

where λ_{ct} is a positive quantity unless $C_4 > 0$, and the contribution to the anharmonicity from the trap imperfection is larger than that from the ion cloud, in which λ_{ct} will be negative.

3 Measurement of anharmonic effects with rf absorption detection

Under the action of a detection voltage $V_d \cos \omega t$ applied to the end caps of the trap, the equivalent circuit is shown schematically in Fig. 2 [23]. It follows that the equation of motion of the ion cloud, when L_0C_0 parallel circuit is tuned to the same frequency as the detecting voltage, is

$$\ddot{z}_c + \gamma \dot{z}_c + \omega_{ct}^2 \left[1 + \frac{8}{3} \lambda_{ct} \left(\frac{z_c}{R_c}\right)^2\right] z_c = \frac{q\kappa}{2mz_0} \frac{V_d \cos \omega t}{1 + R_f G_0}, \tag{17}$$

where $G_0 = 1/R_0$ is the resonant admittance of L_0C_0 parallel circuit; κ is included to account for the fact that the mean detecting field is not simply $V_d \cos \omega t/2z_0$; the damping term is $\gamma = \gamma_1 + \gamma_2$ with $\gamma_2 = 2/\tau_2$ and

$$\gamma_1 = \frac{N}{m} \left(\frac{q\kappa}{2mz_0}\right)^2 \frac{R_f}{1 + R_f G_0}$$

describing the damping of motion due to the collision with the residual gas (τ_2 the phase coherence time) and coupling to the external resistance, respectively. Equation (17) mathematically describes the forced oscillation of the Duffing equation with damping [24].

With an anharmonic term much smaller than the driving term on the right-hand side of (17), the forced oscillation of the ion cloud described by the solution to the equation is still basically harmonic [3], i.e.,

$$z_c = a \cos(\omega t - \psi) \tag{18}$$

with amplitude

$$a^2 = a_m^2 \frac{\gamma^2/4}{[\omega - \omega_{ct}(a)]^2 + \gamma^2/4} \tag{19}$$

and

$$a_m^2 = \left(\frac{q\kappa}{2mz_0\omega\gamma} \frac{V_d}{1 + R_f G_0}\right)^2,$$

$$\omega_{ct}(a) = \omega_{ct}\left(1 + \lambda_{ct} \frac{a^2}{R_c^2}\right).$$

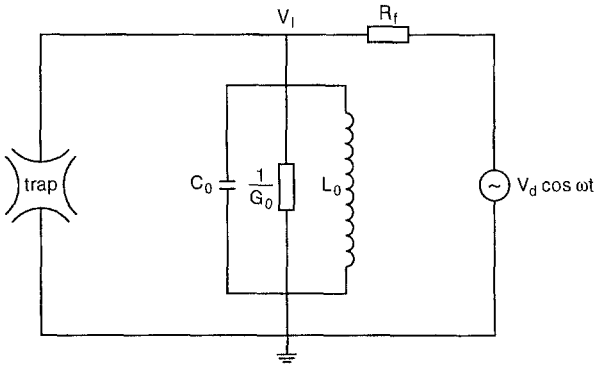

Fig. 2. Equivalent circuit scheme of rf absorption detection

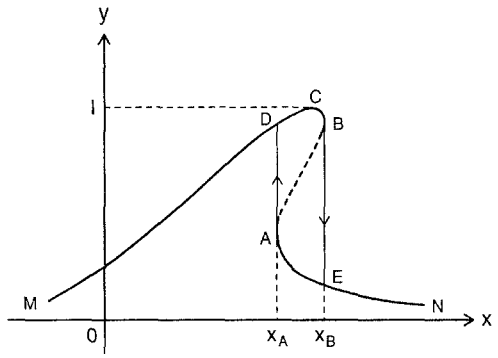

Fig. 3. Hysteresis signal of the trapped ions with rf absorption detection

Because the $\omega_{ct}(a)$ is related to the amplitude of motion, the line shape of a^2 is not Lorentzian but possesses nonlinear characteristics. The motional stability of a single trapped ion in the presence of a small anharmonic potential will generally depend on the magnitudes of the parameters a_z, q_z and the initial position and velocity of the ion. Even with a tiny λ_{ct}, an ion with large values of the initial coordinates in the stability region of (a_z, q_z) may escape from the trap after some time. This stability dependence for a single ion trapped in a new ring trap has been numerically studied in [10]. However, for an ion cloud consisting of ions which have been stably confined (unstable ions excluded), the driven oscillation by the rf detection voltage is stable and shows the relationship between the motion amplitude and frequency as (19) in our case of a minute λ_{ct}.

The movement of the trapped ion cloud will induce a current $i = \kappa N q \dot{z}_c/(2z_0)$ and consequently, energy absorption near resonance. The measured signal $Y = |v_{10}| - |v_1|$ is the difference between the amplitude of voltage v_{10} when there is no ion in the trap and that of the voltage v_1 near resonance (Fig. 2). Transforming kinetic quantities into electric ones, we get

$$Y \approx Y_m \frac{\gamma^2/4}{[\omega - \omega_{ct}(a)]^2 + \gamma^2/4}, \tag{20}$$

with

$$Y_m = \frac{1}{2} \frac{V_d}{1 + R_f G_0} \left[1 - \left(\frac{\gamma_2}{\gamma}\right)^2\right]. \tag{21}$$

The signal is obviously of a line shape similar to a^2.

Introducing the dimensionless parameter η which is analogous to that in [3],

$$\eta = \frac{\lambda_{ct} Y_m \omega_{ct}}{R_c^2 \gamma} \tag{22}$$

it is proved that the line shape of the signal is determined by

$$4\eta^2 y^3 - 4\eta x y^2 + (1 + x^2) y - 1 = 0, \tag{23}$$

with $y = Y/Y_m$ and $x = 2(\omega - \omega_{ct})/\gamma$. When η approaches zero, the line shape reduces to a Lorentzian, but as long as $\eta > 4/(3\sqrt{3}) \approx 0.77$, the line shape of the signal shows hysteresis, a characteristic nonlinear phenomenon as shown in Fig. 3. The signal for sweeping the detection frequency forwards is along the route of points MCBEN but NEADM for sweeping backwards. In other words, the detected signal line shape depends on not only motion parameters of the ion cloud in the trap and the probing conditions but also on the sweeping directions. For different η, the critical points A and B for hysteresis and relative distance $x_B - x_A$ between the descending and ascending edges are calculated in Table 1. When $x = 2\eta$, the signal reaches its maximum value Y_m. In addition, the full width at half-maximum of y, Δx, is equal to 2. From the measured frequencies corresponding to maximum and descending and ascending edges, one can obtain the parameter η and the total central frequency ω_{ct}.

Table 1. Critical hysteresis values for different η

η	x_A	y_A	x_B	y_B	$x_B - x_A$
10	4.98	0.00	20.01	0.999	15.03
9	4.80	0.00	18.01	0.999	13.22
8	4.60	0.103	16.02	0.999	11.42
7	4.38	0.113	14.02	0.998	9.63
6	4.15	0.126	12.02	0.998	7.88
5	3.89	0.143	10.03	0.997	6.15
4	3.57	0.167	8.03	0.996	4.46
3	3.20	0.206	6.04	0.993	2.84
2	2.72	0.279	4.06	0.984	1.34
1	2.00	0.500	2.13	0.920	0.14
0.9	1.89	0.560	1.95	0.891	0.06

In our preliminary experiment [14], the hysteresis of the rf spectra of N_2^+ and Ba^+ were observed. N_2^+ was produced by electron bombarding the background gases and Ba^+ (isotope 137) by heating the platinum filament on which the $Ba(NO_3)_2$ was deposited. We had seen that η and thus λ_{ct} for N_2^+ and Ba^+ were positive and negative, respectively, which implied that C_4 for our trap was positive. For Ba^+, η increased as the confinement voltages V_{dc} and V_{ac} increased under a fixed detection frequency ω(iso-β_z line) or it decreased as V_{ac} increased under a fixed V_{dc}, which was basically in agreement with (7). When the number of the ions was changed by selecting a different heating current or the time delay between the ion production and signal acquisition, we observed the variation of

width and height of the hysteresis signals. Though the operation points were not selected on a spherical pseudopotential line, the variation of η with ion number could be qualitatively explained by (14). From eq (21) and (22), we know that the magnitude of η is proportional to detection voltage V_d and this dependence was noticable in the experiment. These experimental results thus justified, to some extent, our theoretical analyses about the origin of the anharmonic potential in an actual Paul trap. If the values of γ_2, R_c and total ion number N can be extracted from the signal intensity analysis and circuit parameters in eq (21) are known, λ_{ct} will be evaluated from (22). And finally, from (15) and (16) important information about the trap-structure coefficient C, can be derived, in principle, and our model and assumptions can be further checked, which all needs experimental verification.

Conclusion

The extended pseudopotential expression for a Paul trap with an additive octupole potential originating from an imperfect trap configuration is derived. Under the spherical pseudopotential operation condition, the nonlinear terms of the effective potential for a giant particle modeling the ion cloud in a weak probing field are obtained. For a single-species ion cloud in an actual Paul trap both the imperfect trap configuration and the ion-cloud potential are origins of the anharmonicity, which manifests itself in the line shape of the rf resonance signals of the ions. Therefore, some important information of the trap configuration and ion cloud could be extracted by analyzing the features of the line shape. The present study will provide some clues for eliminating the anharmonicity and improving the line shape of the signals, which are of significance for precision measurements and other applications. Furthermore, it will also furnish another means for studying anharmonicity and hysteresis, which are wide-spread in various fields.

Acknowledgements. This work was supported by the Chinese Academy of Sciences and the National Natural Science Foundation of China.

References

1. D.J. Wineland, W.M. Itano, R.S. Van Dyck Jr.: Adv. At. Mol. Phys. **19**, 135 (1984)
2. R. Blatt, P. Gill, R.C. Thompson: J. Mod. Opt. **39**, 193 (1992)
3. L.S. Brown, G. Gabrielse: Rev. Mod. Phys. 58, 233 (1986)
4. R.F. Bonner, J.E. Fulford, R.E. March, G.F. Hamilton: Int. J. Mass Spectrom. Ion Proc. **24**, 255 (1977)
5. G. Gabrielse, F.C. MacKintosh: Int. J. Mass Spectrom. Ion Proc. **57**, 1 (1984)
6. J.D. Prestage, G.J. Dick, L. Maleki: J. Appl. Phys. **66**, 1013 (1989)
7. M.G. Raizen, J.M. Gilligan, J.C. Bergquist, W.M. Itano, D.J. Wineland: J. Mod. Opt. **39**, 233 (1992)
8. M. Tackikawa, M. Kajita, T. Shimizu: IEEE Trans. IM- **42**, 281 (1993)
9. H. Walther: In *Irregular Atomic Systems and Quantum Chaos*, ed. by J.-C. Gay (Gordon Breach, New York 1991)
10. M. Kajita, A.V. Zvyagin: Appl. Phys. B **58**, 295 (1994)
11. A.E. Kaplan: Phys. Rev. Lett. **48**, 138 (1982)
12. G. Gabrielse, H.G. Dehmelt, W. Kells: Phys. Rev. Lett. **54**, 537 (1985)
13. A. Kajita, M. Kimura, S. Ohtani, H. Tawara, Y. Saito: J. Phys. Soc. Jpn. **59**, 1127 (1990)
14. K. Gao, M. Yan, G. Huang, X. Zhu, X. Luo, J. Li, L. Shi: Chin. Sci. Bull. **39**, 1334 (1994)
15. D.J. Wineland, J.J. Bollinger, W.M. Itano, J.D. Prestage: Opt. Soc. Am. B **2**, 1712 (1985)
16. L.S. Cutler, C.A. Flory, R.P. Giffard, M.D. McGuire: Appl. Phys. B **89**, 251 (1986)
17. G.-Z. Li: Z. Phys. D **14**, 1 (1989)
18. R. Blatt, P. Zoller, G. Holtzmuller, I. Siemers: Z. Phys. D **4**, 121 (1986)
19. C. Meis, M. Desaintfuscien, M. Jardino: Appl. Phys. B **48**, 59 (1988)
20. E. Fischer: Z. Phys. D **156**, 1 (1959)
21. N.W. McLachlan: *Theory and Application of Mathieu Functions* (Oxford Univ. Press, Oxford 1947)
22. H.G. Dehmelt: Adv. At. Mol. Phys. **3**, 53 (1967)
23. M.N. Gaboriaud, M. Desaintfuscien, F.G. Major: Int. J. Mass. Spectrom. Ion Phys. **41**, 109 (1981)
24. A.H. Nayfeh, D.T. Mook: *Nonlinear Oscillations* (Wiley, New York 1979)